

NEW MEASUREMENTS OF DIRECT CP VIOLATION*

H. FOX†

Institut für Physik, Johannes Gutenberg-Universität Mainz
D-55099 Mainz, Germany*(Received October 28, 1999)*

After reviewing the theoretical formalism of ε'/ε and the predictions of the Standard Model, I describe the detectors of the NA48 and KTeV collaborations. The analysis methods of the two groups are compared. The two new measurements of the parameter $\text{Re}(\varepsilon'/\varepsilon)$ are presented.

PACS numbers: 11.30.Er

1. Introduction

Since the discovery of CP violation in 1964 [1] the mechanism leading to the phenomenon has been under investigation. So far the neutral kaon system is the only place where CP violation has been observed. The Standard Model explains the observations by the mixing of K^0 and \bar{K}^0 . This is known as indirect CP violation, parametrised by ε . However, the Standard Model also predicts the existence of direct CP violation in the decay amplitude of K^0 and \bar{K}^0 , parametrised by ε' . Evidence for direct CP violation was first found in 1988 by the NA31 collaboration [2]. Until recently this result was not confirmed by other experiments. Only at the beginning of 1999 the experiments KTeV at FNAL and NA48 at CERN confirmed the existence of direct CP violation.

In order to compare these measurements to the Standard Model an introduction into the phenomenology of the kaon system is given in Section 2. As many textbooks and papers give only a very short introduction, most of the steps to get to the measurable quantity R are written explicitly. Then the results of the four groups calculating ε'/ε are explained very briefly.

In Section 3 the detectors and the analysis methods of NA48 and KTeV are described. As the description cannot be complete only a few major

* Presented at the XXIII International School of Theoretical Physics "Recent Developments in Theory of Fundamental Interactions", Ustroń, Poland, September 15–22, 1999.

† Member of the NA48 collaboration.

points are discussed. More detailed descriptions can be found in the original papers [13,14].

2. Phenomenology of the kaon system

As the weak interaction violates strangeness \mathcal{S} the states K^0 and \bar{K}^0 may mix. We can define CP eigenstates as

$$K_1 = \frac{1}{\sqrt{2}}(K^0 + \bar{K}^0) \quad \text{CP} = +1, \quad (1a)$$

$$K_2 = \frac{1}{\sqrt{2}}(K^0 - \bar{K}^0) \quad \text{CP} = -1. \quad (1b)$$

As $\pi^+\pi^-$ and $\pi^0\pi^0$ final states coming from K^0 decays have a CP eigenvalue of +1 the decay $K_2 \rightarrow \pi\pi$ is forbidden if CP symmetry holds.

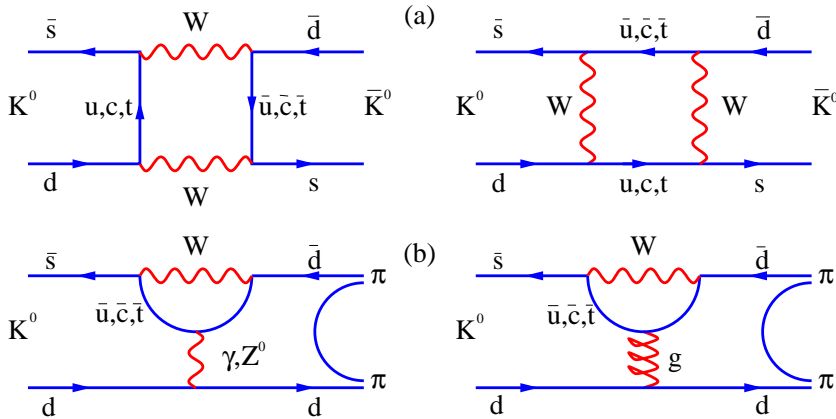


Fig. 1. (a) Box graphs illustrating the $\Delta\mathcal{S} = 2$ mixing between $K^0 \leftrightarrow \bar{K}^0$. (b) Electroweak and gluonic penguin diagrams with $\Delta\mathcal{S} = 1$ which dominate ε' .

Due to the CP violating phase in second order weak transitions with $\Delta\mathcal{S} = 2$ (box diagrams figure 1(a)) the physical eigenstates with defined mass and lifetime differ from the CP eigenstates:

$$K_S = \frac{1}{\sqrt{1 + |\bar{\varepsilon}|^2}} (K_1 + \bar{\varepsilon} K_2), \quad (2a)$$

$$K_L = \frac{1}{\sqrt{1 + |\bar{\varepsilon}|^2}} (K_2 + \bar{\varepsilon} K_1). \quad (2b)$$

In the K^0 - \bar{K}^0 basis we find, with $N_K = \sqrt{2(1 + |\bar{\varepsilon}|^2)}$:

$$K_S = \frac{1}{N_K} [(1 + \bar{\varepsilon})K^0 + (1 - \bar{\varepsilon})\bar{K}^0], \quad (3a)$$

$$K_L = \frac{1}{N_K} [(1 + \bar{\varepsilon})K^0 - (1 - \bar{\varepsilon})\bar{K}^0]. \quad (3b)$$

The contribution of $\bar{\varepsilon}K_2$ to K_S and $\bar{\varepsilon}K_1$ to K_L via mixing is called *indirect CP violation*. The decay of a K_2 or K_1 into a final state of opposite CP via a weak $\Delta S = 1$ transition (penguin diagrams figure 1(b)) is called *direct CP violation* in the decay.

Due to strong interaction between the final state pions additional phases are acquired. The magnitude of these phases depend on the isospin I of the final state. In order to relate CP violation to measurable quantities we thus have to separate the decays into final states with $I = 0$ and $I = 2$. For further discussions we restrict ourselves to final states with two pions. A pion is a boson with isospin $I = 1$, $I_3 = +1, 0, -1$ for π^+ , π^0 , π^- . Using the Clebsch–Gordan coefficients [3] for a $(\pi\pi)_I$ final state, the contributions of $I = 0, 2$ to the charged and neutral final state are:

$$|\pi^+\pi^-\rangle = \sqrt{\frac{2}{3}}|(\pi\pi)_{I=0}\rangle + \sqrt{\frac{1}{3}}|(\pi\pi)_{I=2}\rangle, \quad (4a)$$

$$|\pi^0\pi^0\rangle = -\sqrt{\frac{1}{3}}|(\pi\pi)_{I=0}\rangle + \sqrt{\frac{2}{3}}|(\pi\pi)_{I=2}\rangle. \quad (4b)$$

We can write the decay amplitudes into isospin $I = 0, 2$ final states as

$$\langle(\pi\pi)_{I=0}|H|K^0\rangle = A_0e^{i\delta_0} \quad \langle(\pi\pi)_{I=0}|H|\bar{K}^0\rangle = A_0^*e^{i\delta_0}, \quad \Delta I = \frac{1}{2} \quad (5a)$$

$$\langle(\pi\pi)_{I=2}|H|K^0\rangle = A_2e^{i\delta_2} \quad \langle(\pi\pi)_{I=2}|H|\bar{K}^0\rangle = A_2^*e^{i\delta_2}, \quad \Delta I = \frac{3}{2}. \quad (5b)$$

Here the strong phases $\delta_{0,2}$ are factored out explicitly so that the phases in the amplitudes $A_{0,2}$ are purely weak. Note that the strong phases do not change sign when going from K^0 to \bar{K}^0 whereas the weak phases do.

Now we can express the decay amplitudes A_{+-} and A_{00} of the physical states $K_{S,L}$ into two pions in terms of isospin:

$$\begin{aligned} A_{+-;S,L} &\equiv \langle\pi^+\pi^-|H|K_{S,L}\rangle \\ &= \sqrt{\frac{2}{3}}\langle(\pi^+\pi^-)_{I=0}|H|K_{S,L}\rangle + \sqrt{\frac{1}{3}}\langle(\pi^+\pi^-)_{I=2}|H|K_{S,L}\rangle, \\ A_{00;S,L} &\equiv \langle\pi^+\pi^-|H|K_{S,L}\rangle \\ &= -\sqrt{\frac{1}{3}}\langle(\pi^0\pi^0)_{I=0}|H|K_{S,L}\rangle + \sqrt{\frac{2}{3}}\langle(\pi^0\pi^0)_{I=2}|H|K_{S,L}\rangle. \end{aligned}$$

Using equation (3) one obtains

$$\begin{aligned} A_{+-;S} &= \frac{1}{N_K\sqrt{3}} \left[\sqrt{2}(1 + \bar{\varepsilon})A_0e^{i\delta_0} + \sqrt{2}(1 - \bar{\varepsilon})A_0^*e^{i\delta_0} \right. \\ &\quad \left. + (1 + \bar{\varepsilon})A_2e^{i\delta_2} + (1 - \bar{\varepsilon})A_2^*e^{i\delta_2} \right] \\ &= \frac{1}{N_K\sqrt{3}} \left[\sqrt{2}e^{i\delta_0}(\text{Re } A_0 + i\bar{\varepsilon} \text{Im } A_0) + e^{i\delta_2}(\text{Re } A_2 + i\bar{\varepsilon} \text{Im } A_2) \right]. \end{aligned}$$

Therefore we can write the measurable quantities $\eta_{+-} = \frac{\langle \pi^+ \pi^- | H | K_L \rangle}{\langle \pi^+ \pi^- | H | K_S \rangle}$ and $\eta_{00} = \frac{\langle \pi^0 \pi^0 | H | K_L \rangle}{\langle \pi^0 \pi^0 | H | K_S \rangle}$ as follows:

$$\eta_{+-} = \frac{\sqrt{2}e^{i\delta_0}(\bar{\varepsilon} \operatorname{Re} A_0 + i \operatorname{Im} A_0) - e^{i\delta_2}(\bar{\varepsilon} \operatorname{Re} A_2 + i \operatorname{Im} A_2)}{\sqrt{2}e^{i\delta_0}(\operatorname{Re} A_0 + i\bar{\varepsilon} \operatorname{Im} A_0) + e^{i\delta_2}(\operatorname{Re} A_2 + i\bar{\varepsilon} \operatorname{Im} A_2)}, \quad (6a)$$

$$\eta_{00} = \frac{-e^{i\delta_0}(\bar{\varepsilon} \operatorname{Re} A_0 + i \operatorname{Im} A_0) + \sqrt{2}e^{i\delta_2}(\bar{\varepsilon} \operatorname{Re} A_2 + i \operatorname{Im} A_2)}{-e^{i\delta_0}(\operatorname{Re} A_0 + i\bar{\varepsilon} \operatorname{Im} A_0) - \sqrt{2}e^{i\delta_2}(\operatorname{Re} A_2 + i\bar{\varepsilon} \operatorname{Im} A_2)}. \quad (6b)$$

We can now define ε and ε' as

$$\varepsilon = \frac{\bar{\varepsilon} \operatorname{Re} A_0 + i \operatorname{Im} A_0}{\operatorname{Re} A_0 + i\bar{\varepsilon} \operatorname{Im} A_0} \approx \bar{\varepsilon} + i \frac{\operatorname{Im} A_0}{\operatorname{Re} A_0}, \quad (7)$$

$$\varepsilon' = \frac{1}{\sqrt{2}} \frac{\operatorname{Re} A_2}{\operatorname{Re} A_0} \left(\frac{\operatorname{Im} A_2}{\operatorname{Re} A_2} - \frac{\operatorname{Im} A_0}{\operatorname{Re} A_0} \right) e^{i(\delta_2 - \delta_0)}, \quad (8)$$

$$\omega = \frac{\operatorname{Re} A_2}{\operatorname{Re} A_0} e^{i(\delta_2 - \delta_0)}, \quad (9)$$

ε and ε' are chosen in a way that they reflect the contribution of indirect and direct CP violation. We can choose a phase convention (Wu–Yang phase convention) such that $\operatorname{Im} A_0 = 0$. Then we see from equation (7) that $\varepsilon = \bar{\varepsilon}$ which is the mixing parameter from equation (2). ε has no contribution from the amplitude A_2 and therefore no phase interference. ε measures the amount of indirect CP violation. On the other hand ε' measures the amount of direct CP violation in $\Delta S = 1$ transitions (that is directly in the decay amplitude of the Kaon). It depends on the phase difference in the decay amplitudes A_2 and A_0 . If the phases are identical, ε' vanishes. Incidentally ε and ε' have numerically about the same phase.

Experimentally $|\omega|$ is measured to be 1/22: $\Delta I = 3/2$ transitions are suppressed. This is the $\Delta I = 1/2$ rule. Using these relations we can express equation (6) as

$$\eta_{+-} = \varepsilon + \frac{\varepsilon'}{1 + 1/\sqrt{2}\omega} \approx \varepsilon + \varepsilon', \quad (10a)$$

$$\eta_{00} = \varepsilon - \frac{2\varepsilon'}{1 - \sqrt{2}\omega} \approx \varepsilon - 2\varepsilon'. \quad (10b)$$

From this we can see that (using $\varepsilon' \ll \varepsilon$)

$$R \equiv \left| \frac{\eta_{00}}{\eta_{+-}} \right|^2 \approx 1 - 6 \operatorname{Re} \left(\frac{\varepsilon'}{\varepsilon} \right). \quad (11)$$

Thus the measurement of the double ratio

$$R = \frac{\Gamma(K_L \rightarrow \pi^0 \pi^0) / \Gamma(K_S \rightarrow \pi^0 \pi^0)}{\Gamma(K_L \rightarrow \pi^+ \pi^-) / \Gamma(K_S \rightarrow \pi^+ \pi^-)} \quad (12)$$

gives access to the relative magnitude of direct CP violation.

Reviews and introductory articles about CP violation for further reading can be found in [4].

2.1. Theoretical estimates

Various different methods are used to calculate the value of $\text{Re} \left(\frac{\varepsilon'}{\varepsilon} \right)$. Due to the difficulties in calculating hadronic matrix elements, which involve long distance effects, the task turns out to be very difficult. Several non-perturbative approaches are used to solve the problem. Summaries of the various results can be found in [7, 8]. The following results have been obtained recently (see also [9]):

1. The Dortmund group uses the $1/N_C$ expansion and Chiral Perturbation Theory (χ PT). They quote a range of $1.5 \times 10^{-4} < \varepsilon'/\varepsilon < 31.6 \times 10^{-4}$ [5] from scanning the complete range of input parameters.
2. The Munich group uses a phenomenological approach in which as many parameters as possible are taken from experiment. Their result [6] is $1.5 \times 10^{-4} < \varepsilon'/\varepsilon < 28.8 \times 10^{-4}$ from a scanning of the input parameters and $\varepsilon'/\varepsilon = (7.7_{-3.5}^{+6.0}) \times 10^{-4}$ using a Monte Carlo method to determine the error.
3. The Rome group uses lattice calculation results for the input parameters. Their result is $\varepsilon'/\varepsilon = (4.7_{-5.9}^{+6.7}) \times 10^{-4}$ [10].
4. The Trieste group uses a chiral quark model to calculate ε'/ε . Their result is $7 \times 10^{-4} < \varepsilon'/\varepsilon < 31 \times 10^{-4}$ [8] from scanning.

The scanning method assumes a flat probability within $\pm 1\sigma$ of the theoretical input parameters. It hides the fact that high values of ε'/ε are less probable as all input parameters have to match perfectly.

In general theoretical predictions are lower than the combined experimental result (see figure 6). However, given the enormous difficulties in the calculation, already the agreement in the sign and the order of magnitude is regarded as a success [7]. The theoretical values are within the reach of the experimental results when all input parameters are pushed to the extreme of the allowed limit. But this conspiracy of parameters is seen as unnatural.

2.2. Experimental measurements

Due to the smallness of ϵ'/ϵ also the experimental detection is very challenging. The first evidence for direct CP violation was found by the experiment NA31 in 1988 with $\text{Re}(\epsilon'/\epsilon) = (33 \pm 11) \times 10^{-4}$ [2]. In 1992/93 the experiments NA31 at CERN and E731 at FNAL presented final results which had a probability of only 7.6% to agree. The CERN result [11] of $(23.0 \pm 6.5) \times 10^{-4}$ shows with more than 3σ a clear evidence for direct CP violation while the Fermilab result [12] with $(7.4 \pm 5.9) \times 10^{-4}$ is consistent with zero. The situation has been clarified only at the beginning of 1999 when two new experiments announced their first results. KTeV at FNAL measures $(28.0 \pm 4.1) \times 10^{-4}$ [13] while NA48 at CERN measures $(18.5 \pm 7.3) \times 10^{-4}$ [14]. Now there is general agreement that $\text{Re}(\epsilon'/\epsilon)$ is above zero and direct CP violation exists. Figure 6 gives a summary of the theoretical predictions and the measured values of $\text{Re}(\epsilon'/\epsilon)$. The two new measurements are described in the following.

3. The new measurements of $\text{Re}(\epsilon'/\epsilon)$ by NA48 and KTeV

3.1. Principle of the measurement

As given in equation (12) both experiments measure the four decay modes $K_{S,L} \rightarrow \pi^0\pi^0$ and $K_{S,L} \rightarrow \pi^+\pi^-$. The limiting mode is $K_L \rightarrow \pi^0\pi^0 \rightarrow 4\gamma$ for two reasons. On the one hand these K_L decays are suppressed due to indirect CP violation by 2.3×10^{-3} . On the other hand the neutral final state consists of four particles which decreases the acceptance of the detector with respect to the $\pi^+\pi^-$ final state. To reach the statistical precision of a few 10^{-4} about $4 - 5 \times 10^6$ $K_L \rightarrow \pi^0\pi^0$ decays have to be collected. First results with this accuracy are envisaged for the beginning of the next millenium.

In order to minimise systematic effects all four decay modes are measured simultaneously. The quantities actually measured are the number of decays $N_{S,L}^{+-,00}$ with $N = \Gamma \cdot \Phi \cdot a \cdot \epsilon$. Γ is the branching ratio, Φ denotes the flux of $K_{S,L}$, a is the detector acceptance, and ϵ the trigger efficiency.

To first order trigger efficiencies are identical for K_S and K_L decays ($\epsilon_L = \epsilon_S$). If the fiducial volume and the detector are identical for K_S and K_L decays we also may assume $a_S = a_L$ to a very good approximation.

If the equalities above hold we can relate equation (12) to the measured quantities N by expanding the equation with terms a_L^{00}/a_S^{00} , $\epsilon_L^{00}/\epsilon_S^{00}$ and the charged equivalent:

$$R = \frac{\Gamma_L^{00}/\Gamma_S^{00}}{\Gamma_L^{+-}/\Gamma_S^{+-}} = \frac{\Gamma_L^{00}\Phi_L a_L^{00}\epsilon_L^{00}/\Gamma_S^{00}\Phi_S a_S^{00}\epsilon_S^{00}}{\Gamma_L^{+-}\Phi_L a_L^{+-}\epsilon_L^{+-}/\Gamma_S^{+-}\Phi_S a_S^{+-}\epsilon_S^{+-}} = \frac{N_L^{00}/N_S^{00}}{N_L^{+-}/N_S^{+-}}. \quad (13)$$

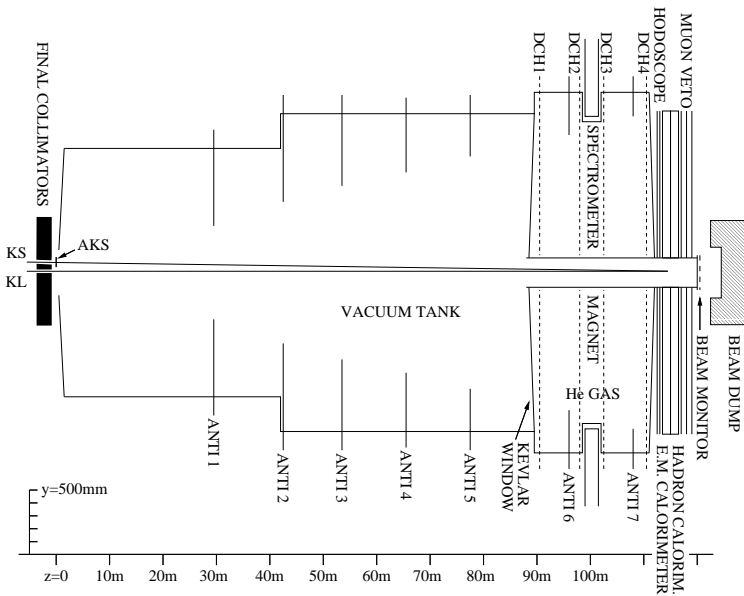


Fig. 2. Layout of the main detector components of the NA48 experiment. Note the different scale in the z and y -axis.

Small deviations from the above stated equalities lead to corrections which have to be applied to the measured raw value of R . These are the main sources of systematic errors.

KTeV has started data taking in 1996 while NA48 followed one year later. The result KTeV has published is based on 25% of their statistics from 1997. A problem in their software level 3 trigger code has made it necessary to use the neutral data from 1996 and the charged data from 1997. However, the result using 1996 data alone, albeit with increased systematic uncertainty, is consistent with the published one. NA48 has published the result of the data taken in 1997.

The analysis is performed in energy bins. In this way small differences in the energy spectrum have no systematic effect as the energy spectrum can be assumed to be flat within one energy bin.

3.2. The NA48 detector

In the design of the NA48 detector the cancellation effect of the double ratio is exploited as much as possible. The key features are (1) two almost

collinear beams which lead to an almost identical illumination of the detector and (2) the lifetime weighting of the events defined as K_L events.

The K_L target is located 126 m upstream of the beginning of the decay region. As the decay lengths at the average kaon momentum of 110 GeV/ c are $\lambda_S = 5.9$ m and $\lambda_L = 3\,400$ m respectively, the neutral beam derived from this target is dominated by K_L . The K_S target is located 6 m upstream of the decay region so that this beam is dominated by K_S . The two beams are almost collinear: The K_S target is situated 7.2 cm above the center of the K_L beam. The relative angle of the beams is 0.6 mrad so that they converge at the position of the electromagnetic calorimeter. Figure 2 shows a schematic layout of the detector.

The beginning of the K_S decay region is defined by an anti-counter (AKS). This detector is used to veto decays occurring upstream. The position of the AKS also defines the global energy scale as the energy is directly correlated to the distance scale (see equation (14)). The decay region itself is contained in a 90 m long evacuated tank.

The beam geometry and the lack of angle information in the calorimeter do not allow one to distinguish between the two targets in the neutral decay mode. A detector (tagger) consisting of an array of scintillators is situated in the proton beam directed to the K_S target. If a proton is reconstructed within a time window of ± 2 ns with respect to a decay, the event is defined as K_S event. The absence of a reconstructed proton defines a K_L event.

A magnetic spectrometer is used to reconstruct $K_{S,L} \rightarrow \pi^+\pi^-$ decays. The spectrometer consists of a dipole magnet with "momentum kick" of 265 MeV/ c and four drift chambers which have a spatial resolution of $\sim 90\mu\text{m}$. This leads to a mass resolution of 2.5 MeV/ c^2 . A hodoscope consisting of two planes of plastic scintillator provides the time of a charged event with a resolution of about 200 ps. The four quadrants of the hodoscope are also used in the trigger for charged events.

A quasi-homogeneous liquid krypton electro-magnetic calorimeter (LKR) is used to identify the four photons from a $\pi^0\pi^0$ event. Liquid krypton has an interaction length of $X_0 = 4.7$ cm which allows one to build a compact calorimeter with high energy resolution ($\Delta E/E = 1.35\%$ measured for electrons coming from a $K_L \rightarrow \pi e \nu$ (K_{e3}) decay) and very good time resolution (< 300 ps). It consists of 13212 2×2 cm² cells pointing to the average K_S decay position. The spatial resolution is better than 1 mm for $E_\gamma > 10$ GeV. At 9.5 X_0 (position of the shower maximum) a hodoscope consisting of scintillating fibres can be used to give an independent trigger.

The electromagnetic calorimeter is complemented by an iron sandwich calorimeter with 6.8 nuclear interaction lengths which measures the remaining energy of hadrons for use in the trigger for charged events.

A muon veto detector, consisting of three planes of scintillator shielded by 80 cm of iron, is used to identify muons to veto $K_L \rightarrow \pi\mu\nu$ ($K_{\mu 3}$) events.

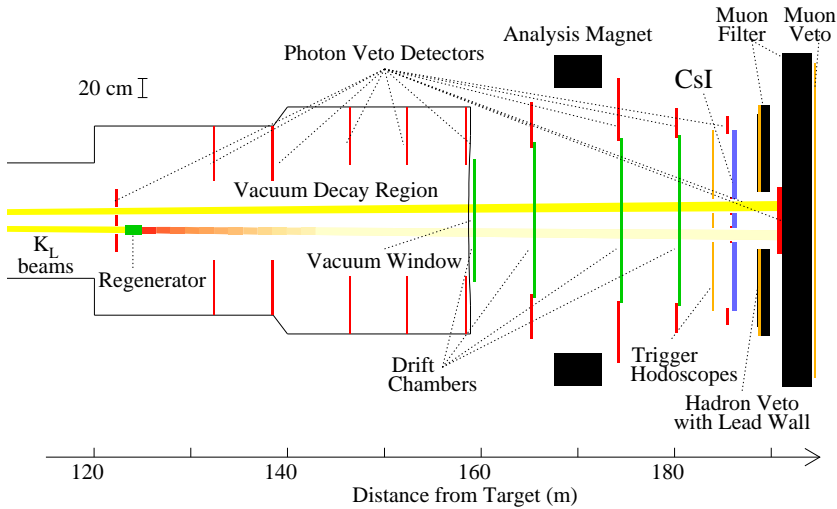


Fig. 3. Layout of the main detector components of the KTeV experiment.

3.3. The KTeV detector

The principle layout of the KTeV detector is similar to NA48 as both experiments work in a similar environment. The main difference is the way K_S are produced.

KTeV uses two well separated kaon beams derived from a single target. This has two advantages: (1) The time structure is identical for both beams. (2) It is possible to distinguish between events coming from either of the beams from the vertex position. Both beams are dominated by the K_L component. The K_S component is produced by coherent regeneration in one of the beams (*regenerator beam*). This beam is attenuated by a movable absorber upstream of the regenerator to yield about the same number of K_S and K_L decays. The regenerator alternates between both beams every minute in order to keep the detector illumination identical for the K_S and the K_L components.

The beginning of the decay region of the regenerator beam is defined by a lead-scintillator counter at the downstream end of the regenerator. The decay region of the vacuum beam starts at a mask anti-counter. The decay region itself is also evacuated.

Similar to NA48 the KTeV spectrometer consists of four drift chambers; the magnet provides a momentum kick of $p_t = 412$ MeV/c, leading to a

mass resolution of $\sigma_{m_{\pi^+\pi^-}} = 1.6 \text{ MeV}/c^2$. For triggering of charged events a scintillator hodoscope is used.

The electro magnetic calorimeter (CsI) consists of 3100 pure Cesium-Iodide crystals with an interaction length of $X_0 = 1.85 \text{ cm}$. In the inner region the size is $2.5 \times 2.5 \text{ cm}^2$ and in the outer region $5.0 \times 5.0 \text{ cm}^2$. The wrapping of the CsI blocks is individually tuned to optimise the energy resolution. Two beam holes of $15 \times 15 \text{ cm}^2$ allow the two kaon beams to pass to the beam dump. Tungsten-scintillator anti-counters (collar anti) define the inner aperture. The energy resolution is 0.75% as measured with K_{e3} decays.

In addition 10 lead-scintillator ‘‘photon veto’’ counters are used to detect particles escaping the decay volume. The background is further reduced by a muon veto counter consisting of 4 m of steel and a hodoscope.

3.4. Data analysis NA48

To identify events coming from the K_S target a coincidence window of $\pm 2 \text{ ns}$ between reconstructed protons in the tagger and the event time is chosen (see figure 4(a),(c)). Due to inefficiencies in the tagger and in the proton reconstruction a fraction α_{SL} of true K_S events are misidentified as K_L events. On the other hand there is a constant background of protons in the tagger which have not led to a good K_S event. If those protons accidentally coincide with a true K_L event, this event is misidentified as a K_S decay. This fraction α_{LS} depends only on the proton rate in the tagger and the width of the coincidence window.

Both effects, α_{SL}^{+-} and α_{LS}^{+-} , can easily be measured (see figure 4(b)) in the charged mode as K_S and K_L can be distinguished by the y -position of the decay vertex. The results are $\alpha_{SL}^{+-} = (1.5 \pm 0.1) \times 10^{-4}$ and $\alpha_{LS}^{+-} = (0.1119 \pm 0.0003)$. This means that about 11% of true K_L events are misidentified as K_S events, however, this quantity is precisely measured to the 10^{-4} level. What is important for the measurement of R is the difference between the charged and the neutral decay modes $\Delta\alpha_{LS} = \alpha_{LS}^{00} - \alpha_{LS}^{+-}$. Proton rates in the sidebands of the tagging window are measured in both modes to measure $\Delta\alpha_{LS}$. The result is $\Delta\alpha_{LS} = (10 \pm 5) \times 10^{-4}$. Several methods have been used to measure $\Delta\alpha_{SL}$, yielding an estimate of $\Delta\alpha_{SL} = (0.8_{-1.0}^{+3.0}) \times 10^{-4}$ (see e.g. figure 4(d)).

Another important correction is the background subtraction. Decays $K_L \rightarrow \pi e \nu$ and $K_L \rightarrow \pi \mu \nu$ can be misidentified as $K \rightarrow \pi^+ \pi^-$ decays, as the ν is undetectable. However, since the ν carries away momentum and energy, these events can be identified by their high transverse momentum p_t' and their reconstructed invariant mass. The remaining background can be measured by extrapolating the shape of the background in the $m - p_t'^2$ -

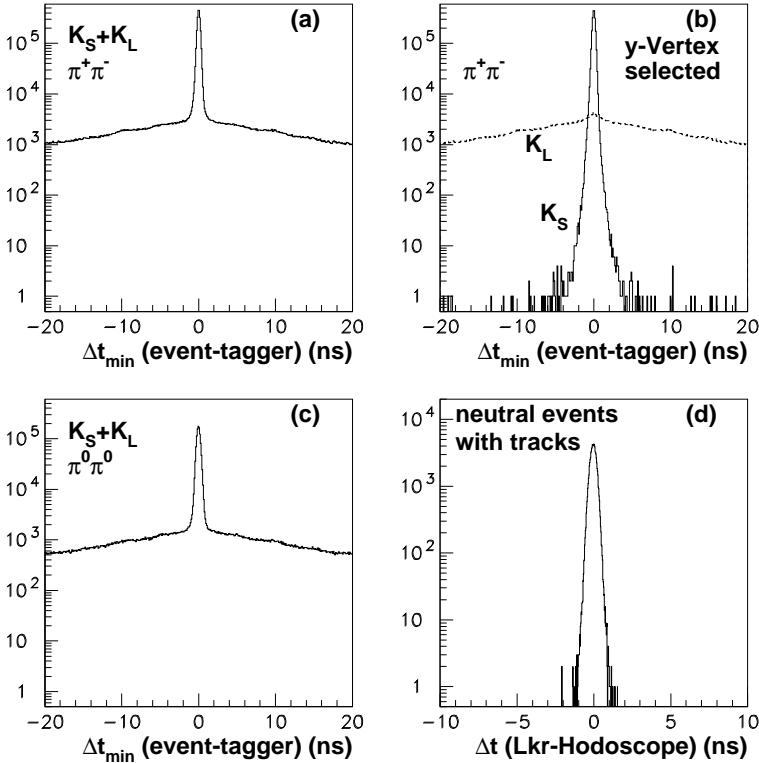


Fig. 4. (a),(c): Minimal difference between tagger time and event time (Δt_{\min}). (b) Δt_{\min} for charged K_L and K_S events. (d) Comparison between charged and neutral event time. For this measurement decays, selected by the neutral trigger, with tracks are used (γ conversion and Dalitz decays $K_S \rightarrow \pi^0 \pi_D^0 \rightarrow \gamma \gamma \gamma e^+ e^-$).

plane into the signal region. In this way the charged background fraction is measured to be $(23 \pm 4) \times 10^{-4}$.

A similar extrapolation can be done in the neutral decay mode. Here the background comes from $K_L \rightarrow 3\pi^0$ decays, where two γ are not detected. This leads to a misreconstruction of the invariant π^0 masses. In this case the background fraction is $(8 \pm 2) \times 10^{-4}$.

The number of signal events after these corrections are summarised in Table I.

The efficiency of the triggers used to record neutral and charged events also have to be determined. Independent triggers are used which accept a downscaled fraction of events. In the neutral decay mode the efficiency is measured to be 0.9988 ± 0.0004 without measurable difference between K_S and K_L decays. The $\pi^+ \pi^-$ trigger efficiency is measured to be $0.9168 \pm$

TABLE I

Event numbers after tagging correction (only NA48) and background subtraction.

Event statistics ($\times 10^6$)					
	NA48	KTeV		NA48	KTeV
$K_S \rightarrow \pi^+ \pi^-$	2.09	4.52	$K_L \rightarrow \pi^+ \pi^-$	1.07	2.61
$K_S \rightarrow \pi^0 \pi^0$	0.98	1.42	$K_L \rightarrow \pi^0 \pi^0$	0.49	0.86

0.0009. Here a small difference between the trigger efficiency in K_S and K_L decays is found. This leads to a correction to the double ratio of $(+9 \pm 23) \times 10^{-4}$. The error on this measurement is dominated by the total number of events registered with the independent trigger. This error is one of the main contributions to the systematic error of the measurement of R .

The distance D from the LKR to the decay vertex is reconstructed using the position of the four γ clusters. The formula used is

$$D = \frac{1}{M_K} \sqrt{\sum_{i,j} E_i E_j r_{ij}^2}, \quad (14)$$

where E_i is the energy of cluster i and r_{ij} the distance between cluster i and cluster j . This formula directly relates the distance scale to the energy scale. It is therefore possible to fix the global energy scale with the measurement of the known AKS position in the neutral decay mode. In addition more checks on the energy scale and the linearity of the energy measurement can be performed, such as the measurement of the invariant π^0 mass and the use of the known position of an added thin CH_2 target (a π^- beam produces $\pi^0 \rightarrow 2\gamma$). The comparison of all methods gives an uncertainty of $\pm 5 \times 10^{-4}$ in the global energy scale.

A very important feature of the NA48 analysis is the weighting of the K_L events. The difference in the lifetime between K_S and K_L events produce a different illumination of the detector: There are more K_L events decaying closer to the detector and they are therefore also measured at smaller radii closer to the beampipe. If the detector efficiency depends on the radius this effect could lead to a bias in the measured value of the double ratio R (see equation (13)). NA48 weights the K_L events according to the measured lifetime such that the distribution of the z -position of the decay vertex of K_S and K_L events are equal. Using this method the influence of detector inhomogenities is minimised and the analysis becomes nearly independent of Monte Carlo methods. In fact the acceptance correction due to small de-

tector differences is quite small. The price to pay for the gain in systematics is the loss in statistics.

Although the acceptance is almost equal there are nevertheless small differences in the beam geometry and detector illumination between decays coming from the K_S and the K_L target. These remaining differences are corrected for with Monte Carlo methods. Using the Monte Carlo to calculate the double ratio R the deviation from the input value 1 is $(29 \pm 12) \times 10^{-4}$.

Table II gives an overview of all corrections and the corresponding systematic error. It should be stressed that many of the systematic errors are also statistical in nature like already stated for the error on the trigger efficiency for charged events. These errors can be reduced significantly in future runs.

TABLE II

Corrections and systematic errors of NA48

Source	Correction	Uncertainty	
	$\times 10^{-4}$	$\times 10^{-4}$	
Charged trigger	+9	23	(stat.)
Reconstruction	–	3	
Tagging dilution	+18	9	(stat.)
Tagging efficiency	0	6	(stat.)
Energy scale, non linearity	–	12	
Charged vertex	–	5	
Acceptance	+29	12	(MC stat.)
$\pi^0\pi^0$ background	–8	2	
$\pi^+\pi^-$ background	+23	4	
Beam scattering	–12	3	
Accidental activity	–2	14	(stat.)
All	+57	35	(stat.)

The result of NA48 using the 1997 data sample is

$$\text{Re} \left(\frac{\epsilon'}{\epsilon} \right) = (18.5 \pm 4.5 \text{ (stat)} \pm 5.8 \text{ (sys)}) \times 10^{-4}. \quad (15)$$

3.5. Data analysis KTeV

KTeV has the same physical background as NA48. The methods to reject background events are in principle the same. To determine the remaining background sideband events are used to normalise the Monte Carlo prediction. The key numbers are: a fraction of 6.9×10^{-4} charged background from

K_{e3} and $K_{\mu 3}$ decays and a fraction of 27×10^{-4} neutral background from $3\pi^0$ decays. An additional source of background is scattering in the regenerator, and, to a lesser extent, in the final collimator. The background levels in the regenerator beam are 107×10^{-4} in the neutral mode and 7.2×10^{-4} in the charged mode. The event numbers after background subtraction can be found in Table I.

The main difference in the analysis techniques of the two experiments is the treatment of the acceptance correction. KTeV is not using event weighting but uses very detailed Monte Carlo studies to correct for detector differences in the K_S and K_L decays. K_{e3} and $3\pi^0$ decays are used to model the detector and the agreement between data and Monte Carlo is very good (see figure 5). This leads to a large correction of $(+231 \pm 13) \times 10^{-4}$ to R . The main source of systematic uncertainty is a slight disagreement between data and Monte Carlo comparison in the $\pi^+\pi^-$ decay mode in the vacuum beam. A slope in the z -vertex distribution of $(-1.60 \pm 0.63) \times 10^{-4} \text{ m}^{-1}$ has been found which is applied as a systematic error.

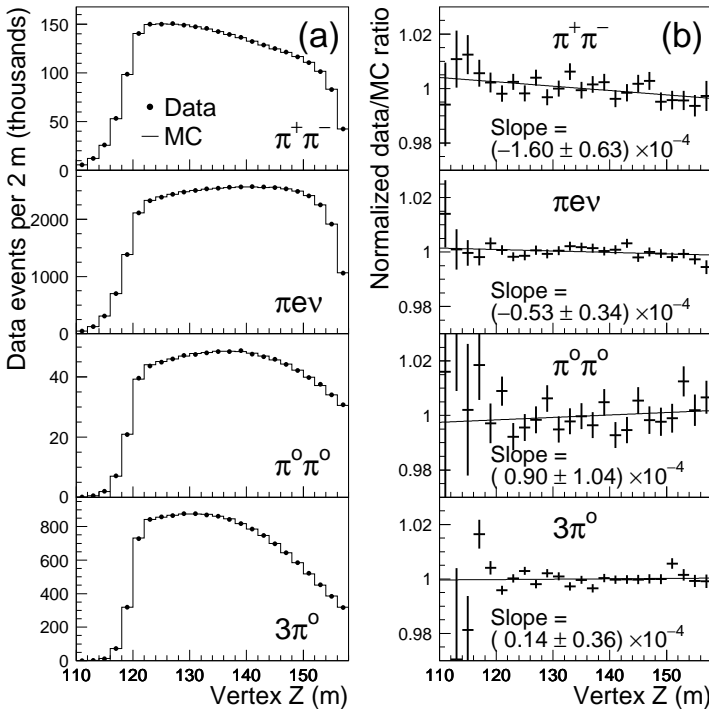


Fig. 5. (a) Distribution of the vacuum-beam Z decay vertex; data (points) and Monte Carlo (histogram). (b) Linear fits to the data/MC ratio of (a).

The energy scale is determined using the known position of the regenerator edge. The comparison of the measured position of the vacuum window with the real position gives an uncertainty of the global energy scale of 4.2×10^{-4} on R . A summary of all systematic uncertainties can be found in Table III.

TABLE III

Systematic uncertainties on R of the KTeV experiment		
Source	Uncertainty ($\times 10^{-4}$)	
	from $\pi^+\pi^-$	from $\pi^0\pi^0$
Trigger (L1/L2/L3)	3.0	1.8
Energy scale	0.6	4.2
Calorimeter nonlinearity	—	3.6
Detector calibration, alignment	1.8	2.4
Analysis cut variations	3.6	4.8
Background subtraction	1.2	4.8
Limiting apertures	1.8	3.0
Detector resolution	2.4	0.6
Drift chamber simulation	3.6	—
Z dependence of acceptance	9.6	4.2
Monte Carlo statistics	3.0	5.4
Regenerator-beam attenuation		
1996 versus 1997		1.2
Energy dependence		1.2
$\Delta m, \tau_S$, regeneration phase		1.2
TOTAL		16.8

The result is obtained by fitting the time distributions of events in the decay region for different kaon energy intervals. These distributions are given by the interference of CP conserving K_S decay amplitudes with CP violating K_L amplitudes and depend on the regeneration amplitude and phase as well as on the relative phases Φ^{+-} or Φ^{00} between the K_S and K_L decay amplitudes. For K_L this leads to the vertex distributions determined by the acceptance variation, as shown in figure 5. Fitting was done “blind”: During the analysis phase, the result of the fit had been covered up by a random offset. The result was only uncovered one week before the result was announced. Given the delicate situation of the previous measurements this was done to exclude any bias by the experimenters.

The result is

$$\text{Re} \left(\frac{\varepsilon'}{\varepsilon} \right) = (28.0 \pm 3.0 \text{ (stat)} \pm 2.8 \text{ (sys)}) \times 10^{-4}. \quad (16)$$

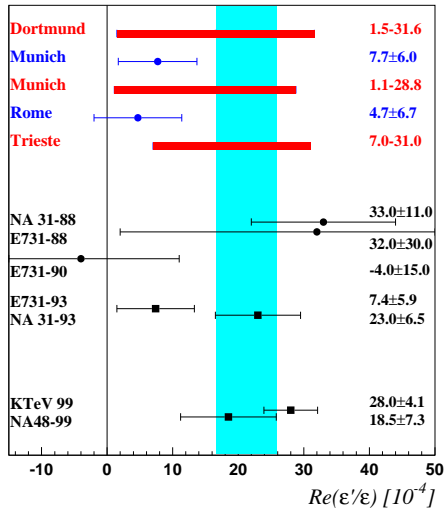


Fig. 6. Theoretical estimates and experimental results of $\text{Re}\left(\frac{\varepsilon'}{\varepsilon}\right)$. The grand average $(21.2 \pm 4.6) \times 10^{-4}$ of the last four experimental results is marked as shaded area. The theoretical estimates shown as bands are a result of a scanning of the input parameters.

4. Outlook

Both experiments have so far analysed only a fraction of their final statistics. The number of events will increase by an order of magnitude. Already now the proof that direct CP violation exists is unambiguous. Both experiments will reach a precision of $\mathcal{O}(10^{-4})$. In addition the third experiment that will measure $\text{Re}(\varepsilon'/\varepsilon)$, KLOE at the Φ -factory DAΦNE in Frascati, Italy, started data taking in 1999. In a few years we will therefore have a very precise experimental result on $\text{Re}(\varepsilon'/\varepsilon)$. In order to fully exploit this measurement the theoretical calculations of ε'/ε within the Standard Model have to improve. Most probably the final answer has to come from lattice calculation. Only then it will be possible to determine whether ε'/ε has another contribution from New Physics beyond the Standard Model.

I wish to thank Prof. K. Kleinknecht and Prof. H. Czyż for giving me the opportunity to give this lecture at Ustron 99. I owe many thanks to V. Martin and Prof. L. Köpke for reading the manuscript. I would also like to thank my colleagues from the NA48 collaboration without whom this lecture would not have been possible.

REFERENCES

- [1] J.H. Christenson, J.W. Cronin, V.L. Fitch, R. Turlay, *Phys. Rev. Lett.* **13**, 138 (1964).
- [2] H. Burkhardt *et al.*, *Phys. Lett.* **B206**, 169 (1988).
- [3] Particle Data Group, *Eur. Phys. J.* **C3**, 183 (1998).
- [4] A. Masiero, CP violation for pedestrians, 1994. European School of High-energy Physics Zakopane, DFPD 94 TH 16; Ling-Lie Chau, *Phys. Rep.* **95**, 1 (1983); G. Buchalla, hep-ph/9707545; B. Winstein, L. Wolfenstein, *Rev. Mod. Phys.* **65**, 1113 (1993); W. Grimus, *Fortschr. Phys.* **36**, 201 (1988).
- [5] T. Hambye, G.O. Köhler, E.A. Paschos, P.H. Soldan, hep-ph/9906434.
- [6] A.J. Buras, M. Gorbahn, S. Jäger, M. Jamin, M.E. Lautenbacher, L. Silvestrini, hep-ph/9904408.
- [7] A.J. Buras, hep-ph/9908395.
- [8] S. Bertolini, M. Fabbrichesi, J.O. Eeg, hep-ph/9802405.
- [9] Two very recent papers should be mentioned: Bardeen *et al.*, see evidence for a large change of one of the hadronic matrix elements in hep-ph/9802300. This would increase ε'/ε significantly; T. Blum *et al.*, have performed a first study of ε'/ε using a new lattice technique. In hep-lat/9908025 they get a large *negative* value for $\text{Re} \left(\frac{\varepsilon'}{\varepsilon} \right)$.
- [10] G. Martinelli, Presentation at Kaon99, Chicago, <http://hep.uchicago.edu/kaon99/talks/martinelli/>
- [11] G.D. Barr *et al.*, *Phys. Lett.* **B317**, 233 (1993).
- [12] L.K. Gibbons *et al.*, *Phys. Rev. Lett.* **70**, 1203 (1993).
- [13] A. Alavi-Harati *et al.*, *Phys. Rev. Lett.* **83**, 22 (1999).
- [14] V. Fanti *et al.*, CERN-EP/99-114, to be published in *Phys. Lett.* **B**.